IJICTR
International Journal of Information & Communication Technology Research

Volume 12- Number 4 – 2020 (33 -45)

# IR-WCO2C: An Enhanced Multi Operators-Based Approach for Content-Aware Image Retargeting

**Mohammadreza Keyvanpour***
Department of Computer Engineering,
Faculty of Engineering,
Alzahra University
Tehran, Iran
keyvanpour@alzahra.ac.ir

**Soheila Mehrmolaei**
Department of Computer Engineering,
Faculty of Engineering,
Data Mining Lab
Alzahra University
Tehran, Iran
s.mehrmolaei@gmail.com

**Hoda Sadaat Ahmadzadeh Hosseini**
Department of Computer Engineering,
Faculty of Engineering,
Alzahra University
Tehran, Iran
h.ahalzahra@gmail.com

Received: 25 September 2019 - Accepted: 16 November 2020

*Abstract*—**In recent years, the image retargeting (IR) problem has been discussed as one of the challenging topics in the field of image processing in different applied domains. In this paper, a multi operators hybrid method is proposed (IR-WCO2C) to improve performance of an IR system, which is performed in three sub-systems. Firstly, the identification precision of important regions is enhanced using a feature extraction technique based on wavelet coefficients (WC) then identified the saliency map of images. In second sub-system, this saliency map is used to improve performance of seam carving process instead of the saliency map identified by conventional methods. Finally, the act of operators selection is improved using metaheuristic techniques to optimize process of operators combination. Findings reveal that our method, IR-WCO2C provided the highest precision (0.74) in the IR process. Also, IR-WCO2C provided an improvement of 20% over the previous methods in different stages of the IR.**

***Keywords*—*Image retargeting; IR-WCO2C; Saliency detection; Multi operators; Metaheuristic.***

## I. INTRODUCTION

Recent advances considering image and video technology disclose the need for electronic devices to adapt images with different displays for showing images according to the size and the aspect ratio of the interest. This problem can be made a new concept, namely image retargeting or IR. The IR means image resizing so that keep useful information and important content of image then present high-quality images according to the desired screen to the user [1, 2]. So far, various techniques have been proposed in this field [3-9], which covered instances of those in the following:

In the last decade, seam carving is considered an excellent content-aware image scaling method,

* Corresponding Author

which is widely used in the IR field. For example, authors in [3] have presented a blind detection based on uniform local binary patterns to detect the seam-carved image. They have adopted SVM as a classifier to train and test features to identify whether an image is subjected to seam carving or not.

In [28], authors proposed multi-operator schemes, namely the MO6 technique, which gave remarkable results in terms of image quality, least distortion, and lowest run-time. They have applied an optimized image distance function, which combines bidirectional image Euclidean distance, dominant color descriptor, and an energy-based coefficient to bypass seams from the point.

Authors in [6] offered a novel method to retarget the original images into different shapes of the image in order to highlight the salient objects of the primary region of the interest, which is named CMAIR (content and mask-aware image retargeting). Also, they have presented a unique irregular interpolation method to produce four possible target images, and an evaluation tool in order to decide the best candidate image as the final output with the consideration of image saliency.

The proposed approach in [7] addressed the image retargeting quality assessment (IRQA) problem with a new framework. This framework is provided based on registration confidence measurement (RCM) and noticeability-based pooling (NBP). Authors have believed that the NBP strategy aggregates the local fidelity of each image block into the overall quality of the retargeted image.

In the other reference, a new framework has been proposed to identify optimally reflected gaps in order to minimize the defined gap of energy using the seam carving method. This framework retained symmetry axes and symmetric objects by adding or removing seam [8].

Authors in [26] proposed a method to accelerate the naive seam carving process by removal or insertion of multiple pixels wide batch seam in a single iteration rather than a single-pixel wide seam. They have believed that the width of a batch seam is a critical factor to make adaptive during the retargeting process in order to preserve the energy of an image. Another property of their method is considered the decrease of the computational time because of the increase of the width of a batch seam.

Authors in the reference [9] have presented an enhanced adaptive image warping approach, which combines with a deep convolutional neural network. This method is generated a visual importance map and a foreground mask map by a pre-trained network. The authors believed that the experiment has shown that their method outperforms current state-of-art image retargeting methods.

In [27], deep Image Retargeting (DeepIR) is presented as a coarse-to-fine framework for content-aware image retargeting. Authors have expressed that a deep convolutional neural network is applied to construct the semantic structure of input images in their method.

The literature review reveals four key points, which have a direct impact on the performance improvement of an IR system. We have remarked these points due to the literature as follows:

- Classifying the previous methods into three classes based on the ahead idea: similarity measure-based methods, continuous mesh deformation-based methods, and insertion and deletion of discrete pixels-based methods [10].
- Popularity and usability multi operators methods in comparison with other methods in the field of IR [11].
- There are major challenges in the previous researches such as creating visual distortion, long time processing, changing image content and quality [12-14].

There is three steps-function in most of the previous methods regarding the IR subject: (1) detecting important regions of the image, (2) running each operator separately, and (3) integrating operators.

In this paper, we have aimed to present an effective hybrid method based on multi operators due to the importance of quality images in current digital devices and advancing technology named IR-WCO2C in order to improve the performance of an IR system and reduce some negative effects of challenges mentioned in the IR subject. Hence, we have listed the paper novelty as follows:

- Proposing an effective multi-operator hybrid method based on three stages: identifying the importance map of the image, operator execution, operator combination.
- Detecting important points or regions of image using wavelet coefficients.
- Improving the performance of traditional seam carving method using wavelet coefficients-based importance map in the seam carving process instead of traditional measures like Energy Gradient.
- Applying optimization algorithms to search the best sequence of operators, providing an appropriate combination of operators, and improving act of this phase.
- To prove the performance superiority of the proposed method in comparison with other traditional methods in the IR field.

The structure of the rest of the paper is organized as follows: the proposed method is presented to improve the performance of an IR system in second section. In the third section, experimental studies are performed then the experiment results are Provided. The performance of the proposed method is evaluated in the fourth section then will discuss comparison results between the proposed method and other conventional methods in this field. Finally, the paper findings are presented in the fifth section and made a possibility for introducing future works.

## II. THE PROPOSED METHOD

In this paper, a new hybrid method is proposed based on multi operators for image retargeting problem named IR-WCO2C, which contains two main components: identifying wavelet coefficients-based important points of image (WC) and optimizing the operators' combination (O2C).

In our research, the proposed method, IR-WCO2C consists of three sub-systems, which are clarified with details in Figure 1.

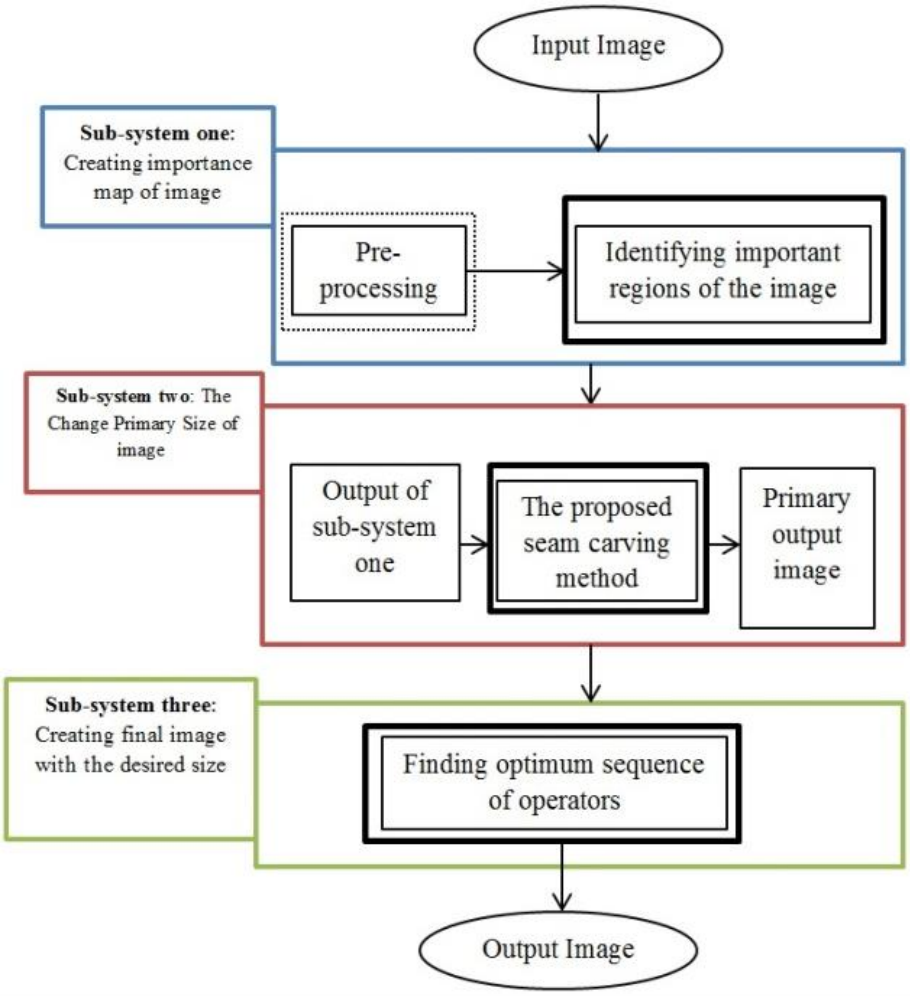


Figure 1. The Schema of the proposed mathod (IR-WCO2C method).

We should mention that the paper innovation has been highlighted by bolded rectangles in the whole of the diagrams. Also, the optional section has specified by a rectangle with round dashes, which are performed when necessary. Each sub-system is explained as follows:

*A. Creating Importance Map of Image*

This sub-system is organized into two phases: "pre-processing" and "identifying important regions of the image". Each part is explained as follows:

*a) Pre-processing:* Pre-processing phase is applied in many of the previous researches regarding IR, which performed conventional noise reduction techniques such as morphology and nonlinear filters in order to reform input images.

Morphology filters are used as a common approach for noise reduction and image reformation in some previous researches but these filters are appropriate to remove specific types of noise and are not consistent for all noise types.

Hence, we have applied the median filter as one of the nonlinear filters to remove noises in the current study, which presented the detail of this filtering in [27]. This nonlinear filter can remove the separate point and the separate linear noises so that do not change image edges [26].

*b) Identifying Important Regions of the Image (I2RI):* Reviewing the previous resources, it can be concluded that exists three main steps for providing feature vector of the interest in most of the previous researches including (1) to separate image to the separable regions, (2) extracting feature from each region separately, and (3) attaining to the final feature vector by applying algebraic operations on each of the extracted feature vectors and integrating those [12, 13]. Therefore, it can be concluded that general process mentioned has high and complex calculations. But this paper has proposed an efficient method based on three-phase (TP) to identify important regions of the image (I2RI), which applies Wavelet transform for this purpose, namely I2RI-TP-WC. In fact, we tried to improve the speed of feature vector extraction by using the proposed approach, I2RI-TP-WC instead of the previously common feature extraction methods. The flowchart of I2RI-TP-WC is shown in Figure 2.

Also, the Pseudocode of I2RI-TP-WC is presented in Figure 3.

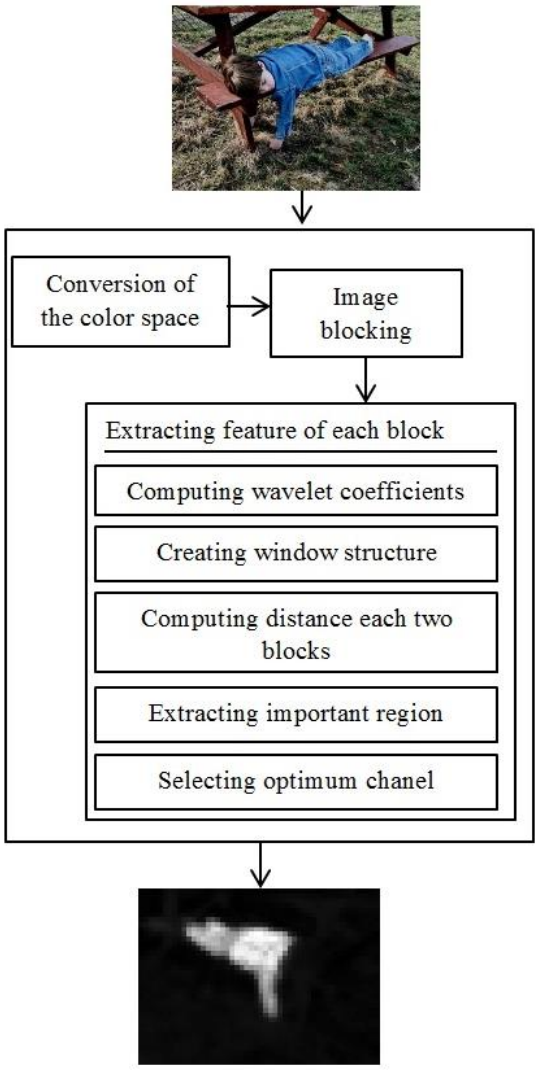


Figure 2. Identifying important regions of image using I2RI-TP-WC

*1)* ***The first phase:*** *Conversion of the color space*

This phase is used the colored models that separated their color and light components to reform image light and contrast through the change of the image light component. In fact, the main motivation for this usage is considered the prevention of the color the creation which not desired inside the image.

*2)* ***Second Phase****:Image blocking*

The act of this phase is considered to divide the input image into 8*8 blocks.

**Algorithm**: I2RI-TP-WC

*Input*: *im*

1: The original image (*im*), is resized.
2: for smoothing texture areas, image is divided into blocks with $n \times n$ pixels.
3: The image is trnasformed from *RGB* space to *LAB* and *YCBCR* space.
4: Calculate *wavelet coefficients* for each block in three layers.
5: Find a window with fixed blocks for each block $(i, j)$. block $(i, j)$ is in the center of the window.
6: Find distance between each two blocks.
7: The attention view is defined as a region with white color as follows:
$s_l^c(p_i) = \frac{1}{l}\sum_{j=1}^{l} w_{ij}^{-1} \times max_{ij}$
8: Calculate $s_l^c(p_i)$ for each block given the output image.

*Output:* important regions of image.

Figure 3. I2RI-TP Pseudocode

*3)* ***Third Phase****: Extracting feature of each block*

In this phase, we have performed the process of the feature extraction using the proposed wavelet transform into five steps as novelty of this phase.

- *Step 1: Computing Wavelet coefficients*

We should note that in most of the previous related work, this step used the energy gradient function instead of wavelet transform-based techniques. A review of the literature shows that much research has been performed on wavelet transform methods and the application of two-dimensional wavelet transform in image and video compression [27-31].

In the following, how to calculate the wavelet coefficients in our method is illustrated in Figure 4.

It has also been found that wavelet transform is more flexible than other transformations such as Fourier transform due to scale-space analysis instead of frequency-time analysis and can be better adapted to the human visual-psychological nature [32]. Since this transform is performed all at once on the whole image, it does not have the negative effects of block-blocking the image. As shown in Figure 5, the wavelet transform coefficients are calculated at three different levels for each block.

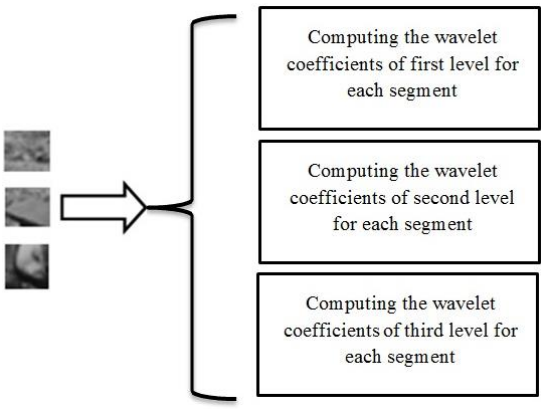


Figure 4. Computing wavelet coefficients in three levels.

- *Step 2: Creating window structure*

In this phase, the window structure with one size has been made to reduce the computational time and improve time and speed of algorithm execution. In fact, the window size is considered one due to the performed tests in the current study. This structure is stated in Figure 5.

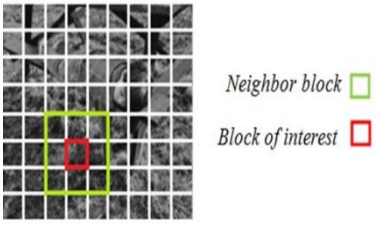


Figure 5. The created window structure.

- *Step 3: Computing distance between two blocks*

This phase has used the Euclidean function for computing distance between the two blocks inside the window space that Pseudocode of this distance is presented in Figure 6.

**Algorithm**: block distance measuring

*Input*: blocks

1: Find the centers of blocks.
2: *for i=1 to block count {*
3: *for j=1 to block count*
4: Calculate Euclidean distance between blocks (*i,j*) as follows:
$w_{i,j} = distance\ (patch_i, patch_j)$
5: *end for}*
6: *end for}*

*Output:* distance between each two blocks.

Figure 6. Pseudocode of the distance computation between blocks.

- *Step 4: Extracting important regions*

In this phase, important regions of the image extract by computing the importance of the desired block (target block). The target block is surrounded by 8 other blocks. For this purpose, a three steps-process is performed.

At first, the internal multiplication between the level 1 wavelet transform of the desired block and the level 1 wavelet transform of one of the adjacent blocks is calculated. This process will then continue for levels two and three. The reason for choosing the internal multiplication operator is to provide better results compared to other operators such as minimum, maximum, wavelet power, etc. Second, the maximum value obtained from these three levels is multiplied by the Euclidean distance between the centers of the two blocks and is summed to the result obtained in the same way from the other window blocks. The distance between the two blocks is calculated as follows.

$$w_{i,j} = distance\ (patch_i, patch_j) \quad (1)$$

In the end, the value of the desired block is obtained as follows:

$$S_l^c = \frac{1}{L \sum_{j=1}^{L} w_{ij}^{-1} * max_{ij}} \quad (2)$$

**Algorithm**: Pixon

*Input*: pixels

1: Start from up on-left pixel.
2: *for each pixel do {*
3: *if pixel is white and the neighbor pixel is white then put this pixel in neighbor ' s cluster.*
4: *if pixel is black and the neighbor pixel is black then put this pixel in neighbor ' s cluster.*
5: *if pixel is white and the neighbor pixel is black then put this pixel in neighbor ' s cluster.*
6: *if pixel is balck and the neighbor pixel is white then put this pixel in neighbor ' s cluster.*
7: return the number of clusters.
8: *end }*

*Output:* number of clusters.

Figure 7. Pseudocode of selecting best channel.

- *Step 5: Selecting optimum channel*

This phase is applied the Pixon structure to select the best channel among six current channels. For this purpose, Pixon images of each channel are constructed based on binary images. Then, the color channel has been selected as the winner channel that has lower Pixon in comparison with other channels. In fact, there is more coherence in the channel with lower Pixon in comparison with other channels. The pseudocode is presented in Figure 7

*B) The Change Primary Size of Image*

So far, different techniques are presented to resize the image that are classified into two classes: resizing based on the content retention and resizing based on without content retention [11, 15].

Seam the carving-based methods can be considered as one of the most famous methods that retain image content when the resizing act is performed on images. The literature review indicated that resizing methods based on content retention is more applicable in the IR problems because of minimizing the modified image degradation in different application areas [32, 33]. It is also shown that what is known as an important and challenging issue in seam carving-based methods is the issue of finding the optimal seam [34].

Hence, we tried to present a new seam carving-based method for changing the primary size of the image due to the applicability and popularity of this class of methods and the current challenge of finding optimum seam, namely the ESC (Enhanced Seam Carving) method. The pseudocode of the ESC method is given in Figure 8.

**Algorithm**: ESC

*Input*: *im* (image)

1: Calculate the energy of each pixel.
2: Find optimum seam by using dynamic programing.
3: Remove the seam from *im*.
4: *if im is not deszired size then recalculate energy function of im and repeat step 2 to 4.*

*Output: im'*

Figure 8. Pseudocode of ESC method.

As is seen in Figure 8, the ESC algorithm applies dynamic programming to find the optimal seam. The output of this subsystem (primary output image) is an image with a size different from the original size, which is created using two operators a) seam carving b) scale. In other words, this subsystem converts the image to the size desired by the user.

The first step of this algorithm is to calculate the energy of each pixel. In the seam carving-based methods, a value is assigned to each pixel which is computed by applying the energy function on the input image. In fact, this value is specified the amount of information that exists in the desired pixel. There are different energy functions that Gradient is one of the usual and popular functions in this field. Literature review [33, 3] and results of experiments in this research have demonstrated the inefficiency of the Gradient function to retain important pixels in the resized images. Thus, we have used the importance map of the image identified through the first sub-system as an energy function instead of the Gradient function in this research.

The next step of the algorithm is to find the optimal seam. The optimal seam is a seam that passes from the least important areas of the image. As shown in Figure 8, the next steps include removing the seam and examining the need to repeat the above steps. As is observed in Figure 8, dynamic programming is applied to find the optimum seam. For this purpose, the cost function is computed by using the energy difference of each pixel and neighboring pixels after determining image energy. After computing the cost matrix, the minimum seam is specified by a backward motion in dynamic programming. For this purpose, at first, a pixel is selected, which have a minimum value in the cost matrix then the whole seam is identified by the energy function of backward-based dynamic programming as follows:

$$M(i,j) = e(i,j) + min\begin{cases} M(i-1,j-1) + C_L(i,j) \\ M(i-1,j) + C_U(i,j) \\ M(i-1,j+1) + C_R(i,j) \end{cases} \quad (3)$$

Where $M$ is matrix that M size is considered the size of input image, $M(i,j)$ is a element of this matrix, $C(i,j)$ shows minimum cost of seam from the first row to $M(i,j)$. At each step, we are looking for a seam that after removing it, the energy added to the image is minimal. In fact, after removing the pixels on a seam, the surrounding pixels, which were not adjacent to each other before the seam was removed, become neighbors, creating a new edge in the image that may cause undesirable effects in the image. Dynamic programming function is depicted to find the optimum seam in Figure 9.

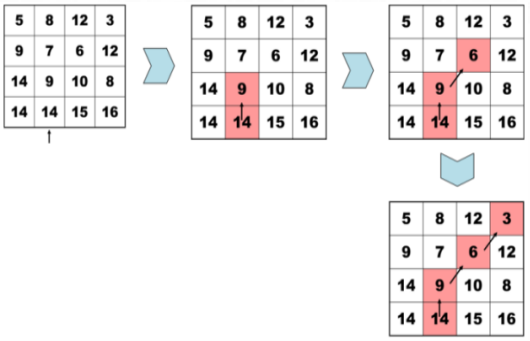


Figure 9. Dynamic programing function for finding of the optimum seam.

After all cost functions have been quantified, the minimum seam is determined by a backward motion, from the end edge to the top edge. First, the pixel is selected with the lowest value in the cost matrix, then the whole seam is identified with the help of dynamic programming. The dynamic programming approach works as a method of dividing and solving based on dividing the problem into subproblems.

*C) Creating Final Image with Size of Interest*

The study of the recent resources discloses popularity of methods based on multi operators among researchers for the IR problems [4, 14, 35-37]. This finding is reasonable and logical since the single operator methods can not present only acceptable results in the field of IR in all application areas.

Hence, the usage of the multi operators' methods can be considered as an apposite solution to improve the performance of an IR system in different application areas. The act of operators combination is performed by using a sequence, namely “multi operators sequence”.

Each operator can be located several times in different positions of a sequence. In this way, the different permutations of operators can be constructed several sequences through operators' combination of seam carving, scaling, and cropping [11].

Despite the successful application of multi-operator methods in the field of IR, there are two challenging problems in the previous researches: how to select an optimum point of operator's replacement and how to achieve an optimal combination of operators [2]. Also, the study of previous researches shows that the frequency of use of each operator and the order of using operators can play an important role to improve the performance of an IR system [25]. Hence, we aim to propose using metaheuristic algorithms to reduce the negative effects of these challenges in this field. For this purpose, we present the Ga-BOS method to

attain the best sequence of operators (BOS). Also, in the process of combining the operators, seam removal operators and uniform scaling were used to re-target the image. The Ga-BOS Pseudocode is given in Figure 10.

As is observed in Figure 10, the Ga-BOS method has applied a Genetic algorithm (Ga) on the second sub-system outputs. In fact, the third subsystem applies the genetic algorithm to the output of the second subsystem in order to find the best sequence of operators and then combining those. Ga tries to provide an optimal or close answer to the optimal. The search operation in this algorithm is performed by a set of points, the number of which can also be a challenge in this area. Because high populations complicate calculations and increase the speed of achieving the optimal answer. Also, this algorithm uses the value of the function in different parts of the search space and does not need to know the derivative of the function or other information from the function. In the Ga-BOS method, each gene has shown iterations number of using operator, the population size is considered 20. Also, the value of crossover and mutation operators are adjusted at 80% and 7%, respectively in this study.

**Algorithm**: Ga-BOS

*Input*: *n, x, μ*

// **Initialize generation 0:**
1: *K:=0;*
2: $P_k$:= a population of *n* randomly-generated individuals*;* Half of the generation is seam carving-scaling and half of the other is scaling-seam carving.
// **Evaluated $P_k$:**
3: Compute fitness (*i*) for each *i*∈ *Pk*:
4: *do* {
// **Create generation k+1:**
// **1. Copy:**
5: Select (*1-x*) × *n* members of $P_k$ and insert into $P_k$;
// **2. Crossover:**
6: Select *x* × *n* members of $P_k$ ; pair them up; produce offspring; insert the offspring into $P_k$+1;
**//3. Mute:**
7: Select μ× *n* members of $P_k$ +1; invert a randomly-selected bit;
**//4. Evaluated $P_k$+1:**
8: Computed fitness (*i*) for each *i*∈ *Pk* ;
//**5. Increment:**
9: *k:=k+1;*}
10: while fitness (A-DTW) of fittest individual is *Pk* is not high enough;
*Output:* fittest individual from $p_k$

Figure 10. The Ga-BOS pseudocode

As is seen in Figure 10, a bi-directional warping function (BDW) is used as a fitness function in the presented Ga-BOS method. The BDW function can be considered as an appropriate way to compute the distance between images with the same height in the semi-automatic IR problems, which measured the similarity between images based on Asymmetric Dynamic Time Warping (A-DTW). The pseudocode of A-DTW$_{max}$ (*s, t*) is given in Figure 11. The A-DTW function is applied to the outcome of operators combination to find the most similarity between the original image and the modified image, and attain the optimum combination of operators. Therefore, similarity measure of image is computed due to the A-DTW (*s, t*) as follows:

$$BDW\left(S,T\right)=max\left\{A-DTW\left(S_i,T_i\right)\right\}+ max\left\{A-DTW\left(T_i,S_i\right)\right\} \quad (4)$$

Where $S_i$ and $T_i$ are $i^{th}$ of row in images *S* and *T*, respectively. A-DTW and BDW computation can be performed in the pixel and patch level.

## III. EXPERIMENTAL STUDIES

We have considered four parts to evaluate the performance of the proposed method in comparison with other the conventional and the related methods in the IR field, which include "Data set", "Metrics of performance evaluation", and "Experiment results and parameters setup", and "visual comparing methods". Each part is clarified with detail in the following.

**Algorithm**: A-DTW$_{max}$

*Input*: $s[1..|s|],\ t[1..|t|]$
//**Calculating pixel mapping**
1: Allocate $M[|s|+1][|t|+1], P[|s|+1][|t|+1]$
2: M[0,0] ≔ 0;
3: *for i:=1 to |s| do*
4: $M[i,0]=\infty$
5: *for j:=1 to |t| do*
6: $M[0,j]=0$
7: *for i:=1 to |s| do*
8: : *for j:=1 to |t| do*
9: $M[i,j] \coloneqq \min\{[M(i,j-1), M(i-1,j)] + d(s[j], t[j])\}$
10: $if\ M[i,j]=M[i,j-1]$
11: $p[i,j]=0$
12: *else*
13: $p[i,j]=1$
// **Back track for maximal difference between the match pixel pairs**
14: $i \coloneqq |s|+1;\ j \coloneqq |t|+1; maxd \coloneqq 0;$
15: *while (i>0)*
16: *temp:=d(s[i],t[j]);*
17: *if p[i,j]=1*
18: if *maxd<temp*
19: *maxd:=temp;*
20: *i:=i-1;*
21: *else*
22: *j:=j-1;*
*Output: maxd*

Figure 11. Pseudocode of A-DTWmax (s, t)

### A. Data set

In this paper, the proposed method is applied to the "MSRA" data set that was collected from http://mmcheng.net/msra10k site. Literature has revealed that the MSRA data set is widely used as a standard data set in many recent and valid resources in order to evaluate methods performance in the IR

field [3, 15-24]. The MSRA data set contains 1000 color images that images do not belong to the specific class. We should mention that "Retarget me" data set is also used to evaluate methods efficiency in terms of operators combination.

*B. Metrics of Performance Evaluation*

In this study, we have used three measures to evaluate the performance of the proposed method, which include "Precision", "Recall", and "F-measure". These metrics are widely used for evaluating methods performance and comparing methods with others in most of the valid previous researches [3, 7, 16, 17]. Precision, Recall, and F-measure are computed, respectively by Equations below:

$$Precision = \frac{\sum_x g_x s_x}{\sum_x s_x} \quad (5)$$

$$Recall = \frac{\sum_x g_x s_x}{\sum_x g_x} \quad (6)$$

$$F_\beta = \frac{\left(1+\beta^2\right) precision * recall}{\beta^2 * precision + recall} \quad (7)$$

Where $g$ and $s$ are the importance maps of the binary masks and the detected importance map, respectively. Also, $\beta$ is a positive parameter to decide the importance of precision over recall in computing the F-measure, which adjusted $\beta^2 = 0.3$.

*C. Experiment results and Parameters setup*

In this section, we have evaluated the performance of the proposed method and adjusted primary parameters of our method such as the window size, the block size, and the wavelet level. For this purpose, some experiments are designed then each experiment is separately performed. In the end, experiment results are reported for each case.

*a) the First Experiment*: In this experiment, we aim to set the window size and block size parameters to the proposed method. For this goal, we have performed our method for different window and block sizes then evaluated performance of our method in terms of precision, recall, and F-measure metrics for each size. The statistical information of parameters is presented in Table 1.

TABLE I. STATISTICAL INFORMATION OF PARAMETERS

| No. | Block size | Window size |
|---|---|---|
| 1 | 8 | 1, 3, 5 |
| 2 | 16 | 1, 3, 5 |
| 3 | 32 | 1, 3, 5 |
| 4 | 64 | 1, 3, 5 |

The evaluation result of the efficiency of the proposed method is reported for different window and block sizes in Figure 12.

As is seen in Figure 12, the best performance is provided by the proposed method in terms of all three metrics when 1 and 8 values are considered to the window size and block size parameters, respectively. Furthermore, the lowest performance is presented in terms of all three metrics when 3 and 64 values are assigned to the window size and block size parameters, respectively. Also, it is observed in Figure 12 that the precision and F- measure metrics have reduced when the increase of window size and block size parameters.

Thus, it can be concluded that the size increase of these parameters has a direct impact on the efficiency reduction of the proposed method. On the other hand, the recall metric increased with the increase of the block size when 1 value assigned to the parameter of the window size.

By comparing values of the recall metric for the window size=2 and 3, it can be said that the mentioned metric increases with the increase of the block size. But the value of this metric has reduced in the next increase of block size (block size=32). Therefore, the reason for the reduction of this metric can be considered the increase of the block size in the situation that the parameter of the window size is considered the same in this experiment (window size=2, 3).

As a general result of this part experiment, it can be said that 1 and 8 values are assigned to the window size and block size parameters in this research work.

*b) the Second Experiment*: In the next experiment, the efficiency of the proposed method is investigated for different values from wavelet levels when window size and block size parameters are considered 1 and 8 (according to the obtained result in the first part of the experiment), respectively. Evaluation results are shown in Table 2.

TABLE II. EVALUATING THE PERFORMANCE OF OUR METHOD FOR DIFFERENT WAVELET LEVELS (MSRA DATA SET)

| Parameters | | Performance | | |
|---|---|---|---|---|
| Window size=1 ; block size=8 | Wavelet level | precision | recall | F-measure |
| | 1 | 0.6732 | 0.7265 | 0.6773 |
| | 2 | 0.6921 | 0.7231 | 0.6946 |
| | **3** | **0.7539** | **0.8153** | **0.74** |

As is seen in Table2, better results are presented for the performance metrics when the proposed method is performed for the wavelet level=3.

As is observed in Table 2, the performance of the proposed method is increased by the addition of

the wavelet levels in terms of precision, recall, and F-measure metrics. Also, the best performance is provided by the proposed method in the third level of the wavelet. By comparing the presented results in Figure 12 and Table 2, it can be concluded that the best performance is given by the proposed method for block size=8, window size=1, and wavelet level=3.

Also, the obtained improvement is computed 11.98%, 12.2%, and 9.2% in the third wavelet level in compared first wavelet level in terms of precision, recall, and F-measure metrics, respectively.

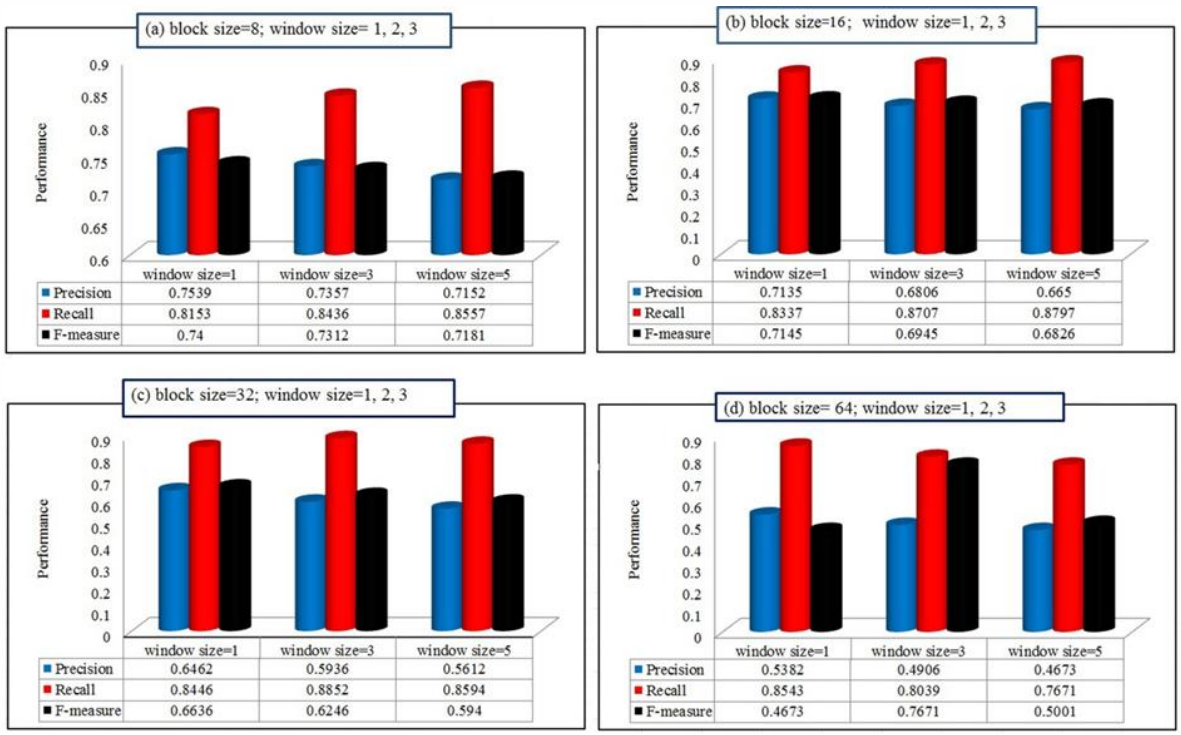


Figure 12. Evaluation result of efficiency of the IR-WCO2C method for the MSRA data set. (a) block size considered 8kb; (b) block size considered 16kb; (c) block size considered 32kb; (d) block size considered 64kb.

## IV. Comparing Methods and Discussion

In this section, we compare the performance of the proposed method with some of the previous methods such as SVA [18], FT [19], GVS [20], HVSAS [15], SDCD [3], L2FWT [16] in the field of IR then comparison results are discussed. This comparison is provided based on two aspects "identifying the importance map of image" and "combining operators" in terms of performance indicators.

### *A. Comparing Performance of methods based on the First Aspect*

This sub-section is presented evaluation results given the variable threshold of the saliency map. at first, the saliency maps are divided into the salient components due to the variable threshold then efficiency of methods is computed for different thresholds. These maps have extracted by our method and SVA [18], FT [19], GVS [20], HVSAS [15], SDCD [3], L2FWT [16], Ch. *et al*. [6], P. *et al*. [7], and Z. *et al*. [35] methods. The variable threshold is computed as follows:

$$T_a = \frac{2}{N} \sum_{\forall p \in I} sal\left(p\right) \quad (8)$$

The threshold values depend on the saliency value of each map created in the variable threshold.

Where *N* is pixels set of the saliency map, *sal (p)* is the saliency value of *P* pixel in the saliency map.

The precision, recall and F-measure metrics have been computed as performance indicators then the precision-recall graph, and F-measure are depicted in Figure 13.

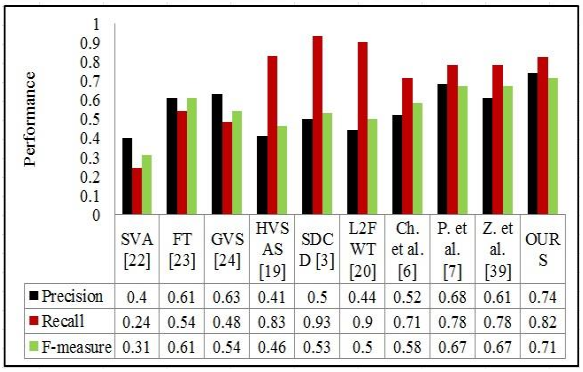


| | SVA [22] | FT [23] | GVS [24] | HVS AS [19] | SDC D [3] | L2F WT [20] | Ch. et al. [6] | P. et al. [7] | Z. et al. [39] | OUR S |
|---|---|---|---|---|---|---|---|---|---|---|
| Precision | 0.4 | 0.61 | 0.63 | 0.41 | 0.5 | 0.44 | 0.52 | 0.68 | 0.61 | 0.74 |
| Recall | 0.24 | 0.54 | 0.48 | 0.83 | 0.93 | 0.9 | 0.71 | 0.78 | 0.78 | 0.82 |
| F-measure | 0.31 | 0.61 | 0.54 | 0.46 | 0.53 | 0.5 | 0.58 | 0.67 | 0.67 | 0.71 |

Figure 13. Comparing performance of methods for variable threshold of saliency map (MSRA data set).

As is reported in Figure 13, the highest precision is provided by the proposed method to detect saliency maps when using the variable threshold compared to those other methods for the MSRA data set. Also, it is seen that the lowest recall is presented by the proposed method in comparison with the SDCD method [3] which is logical. Because sometimes is detected salient pixels instead of salient components by the proposed method. In other words, the identified salient pixels cannot cover fully the salient components. This problem is caused that the lower recall is provided by the proposed method over the SDCD method [3].

As is seen in Figure 13, the proposed method is provided higher precision than Ch. et al. [6] so that the amount of improvement achieved is reported 38%. This finding is clear because Ch. et al. [6] retarget the original images into different shapes to highlight the salient objects of the primary region of interest, while our method uses dynamic programming concepts to detect salient objects in the seam carving step.

Also, evaluation results are shown that our method obtained an improvement of about 10% and 23% in comparison with P. et al. [7] and Z. et al. [34] methods, respectively. This improvement is obvious and logical because optimization algorithms do not play a role in these two approaches, while our approach uses the benefits of optimization techniques to improve the performance of an IR system and increase the quality of the output image.

*B. Evaluating Performance based on the Second Aspect*

In this sub-section, we would like to evaluate the performance of the proposed method in comparison with uni-operator-based methods such as ICA-IR [2], DH-IR [5], and GVS [20]. We should mention that the Retarget me data set used in this part. The implementation and comparison results are depicted in Figure 14.

In the performed comparison, we aim to reduce images width by about 50%-70% by the proposed method and other methods of understudy.

As is seen in Figure 14, the salient components of images are compressed by ICA-IR [2]. This resizing is logical because this research uses the uniform scale method thus the whole of input image components be distorted in the IR process.

Also, it is observed from Figure 14 that the discrete distortions were made in the resized images by DH-IR [5]. These discrete distortions are reasonable because this reference applied the seam carving method for the change of image size. The seam carving contains the minimum value of energy in the whole input image in each step.

Thus, jag edges were made in the output image by DH-IR [5].

Comparing results in Figure 14, it is shown that the GVS method [20] has the ability the distribution the distortion in different directions of the changed image. This result is logical because the GVS method uses a scale-and-stretch warping-based method in the process of image resizing.

Generally, the comparison of the presented results in Figure 14 has demonstrated that the proposed method provided the capability of primary image resizing with fewer distortion and made the most similarity between the original image and the modified image in comparison with other methods.

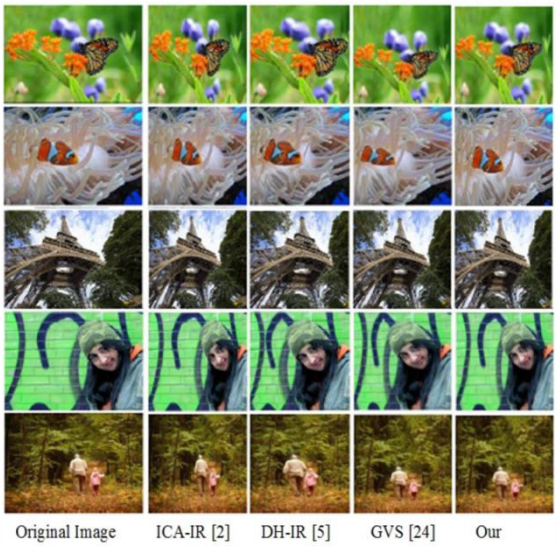


Figure 14. Comparing performance uni-operator-based methods and the proposed method based on combining operators (Retaget me data set).

## V. Conclusion and Future Works

Image retargeting is considered as one of the active research directions in the field of image processing which literature review appears major challenge in this field. In this research, a new hybrid method is presented, namely IR-WCO2C because of significant advances in technology, current challenges, and the importance of using new techniques to present transparent images in the image retargeting problem. IR-WCO2C method

provided the possibility of feature extraction by using wavelet coefficients and replacing Gradient Energy Function instead saliency map identified for seam carving and optimize operators combination.

Also, in this study, the comparison possibility of the proposed method and other methods is provided in this field, which evaluation results assert performance the superiority of the proposed method in the image retargeting problem. In the following, instances of future research topics are listed:

(1) Using neural networks to extract important image regions.

(2) Integrating metaheuristic and computational intelligence-based techniques for presenting better images.

## REFERENCES


[1] Y. Liang, Y.J. Liu, and D. Gutierrez, "Objective quality prediction of image retargeting algorithms". IEEE transactions on visualization and computer graphics, vol. 23, pp.1099-1110, 2016.

[2] S. Wang and A. Abdel-Dayem, "Integrated content-aware image retargeting system". Int. J. Multim. Ubiqu. Eng, vol. 7, pp. 1-16, 2012.

[3] D. Zhang, G. Yang, F. Li, j. Wang, and A.K. Sangaiah, "Detecting seam carved images using uniform local binary patterns. Multimedia Tools and Applications", vol. 79, no. 13, pp. 415-8430, 2020.

[4] Y. Zhang, W. Lin, Q. Li, W. Cheng, and X. Zhang, "Multiple-level feature-based measure for retargeted image quality". IEEE Transactions on Image Processing, vol. 27, pp. 451-463, 2017.

[5] W.P. Fang, W.C. Peng, Y.J. Hu, C. Li, and S.K. Chen, "A Data Hiding Method for Image Retargeting". In Genetic and Evolutionary Computing, 2015, pp. 301-308. Springer, Cham.

[6] H.H. Chang, T.K. Shih, C.K. Chang, and W. Tavanapong, "CMAIR: content and mask-aware image retargeting". Multimedia Tools and Applications, vol. 78, no. 15, pp.21731-21758, 2019.

[7] Y. Niu, S. Zhang, Z. Wu, T. Zhao, W. and Chen, W., "Image Retargeting Quality Assessment Based on Registration Confidence Measure and Noticeability-based Pooling". IEEE Transactions on Circuits and Systems for Video Technology, 2020, PP.1-10.

[8] D. Patel, R. Nagar, and S. Raman, "Reflection symmetry aware image retargeting". Pattern Recognition Letters, vol. 125, pp.179-186, 2019.

[9] J. Wu, R. Xie, L. Song, . and B. Liu, "Deep Feature Guided Image Retargeting". In 2019 IEEE Visual Communications and Image Processing (VCIP) (pp. 1-4). IEEE, 2019.

[10] J. Kiess, S. Kopf, B. Guthier, and W. Effelsberg, "A survey on content-aware image and video retargeting". Acm Transactions on Multimedia Computing, Communications, and Applications (TOMM), vol. 14, no. 3, pp.1-28, 2018.

[11] Z. Qiu, T. Ren, Y. Liu, J. Bei, and Y. Yang, "Multi-operator image retargeting based on automatic quality assessment", Proc. Seventh International Conference on Image and Graphics, 2013, pp. 428-433.

[12] F. Alamdar and M. Keyvanpour, "A new color feature extraction method based on QuadHistogram". Procedia Environmental Sciences, vol. 10, pp. 777-783, 2011.

[13] Y. Li, L. Guo, and L. Jin, "A Content-Aware Image Retargeting Quality Assessment Method Using Foreground and Global Measurement". IEEE Access, vol. 7, pp.91912-91923, 2019.

[14] M. Rubinstein, A. Shamir, and S. Avidan, "Multi-operator media retargeting". ACM Transactions on graphics (TOG), vol. 28, no. 3, pp.1-11, 2009.

[15] Y. Fang, W. Lin, B.S. Lee, C. T. Lau, Z. Chen, and C. W. Lin, "Bottom-up saliency detection model based on human visual sensitivity and amplitude spectrum". IEEE Transactions on Multimedia, vol. 14, no. 1, pp.187-198, 2011.

[16] N. Imamoglu, W. Lin, and Y. Fang, "A saliency detection model using low-level features based on wavelet transform". *IEEE transactions on multimedia*, *vol. 15*, no. 1, pp.96-105, 2012.

[17] Y.Y. Zhang, X.Y. Liu, and H.J. Wang, "Saliency detection via two-directional 2DPCA analysis of image patches". Optik, vol. 125, no. 24, pp.7222-7226, 2014.

[18] L. Itti, C. Koch, and E. Niebur, "A model of saliency-based visual attention for rapid scene analysis", IEEE Transactions on pattern analysis and machine intelligence, vol. 20, no. 11, pp.1254-1259, 1998.

[19] R. Achanta, S. Hemami, F. Estrada, and S. Susstrunk, "Frequency-tuned salient region detection". In IEEE conference on computer vision and pattern recognition, pp. 1597-1604, 2009, IEEE.

[20] J. Harel, K. Christof, and P. Pietro, "Graph-based visual saliency", 2007, PP. 545-552.

[21] A. Borji and L. Itti, "Exploiting local and global patch rarities for saliency detection", In IEEE conference on computer vision and pattern recognition, 2012, pp. 478-485. IEEE.

[22] Y. S. Wang, C. L. Tai, O. Sorkine, and T. Y. Lee, "Optimized scale-and-stretch for image resizing". In ACM SIGGRAPH Asia 2008 papers, 2008, pp. 1-8.

[23] D. Patel and S. Raman, "Accelerated seam carving for image retargeting". *IET Image Processing*, *vol. 13*, no. 6, pp.885-895, 2019.

[24] J. Lin, T. Zhou, and Z. Chen, "Deepir: A deep semantics driven framework for image retargeting". In Proceeding of IEEE International Conference on Multimedia & Expo Workshops (ICMEW), 2019, pp. 54-59. IEEE.

[25] R. Arya, R. K. Agrawal, and N. Singh, "A novel approach for salient object detection using double-density dual-tree complex wavelet transform in conjunction with superpixel segmentation". Knowledge and Information Systems, vol. 60, no. 1, pp.327-361, 2019.

[26] R. Zhu and Y. Wang, "Application of improved median filter on image processing". journal of computers, vol. 7, no. 4, pp.838-841, 2012.

[27] S. Zhang, X. Li and C. Zhang, "Modified adaptive median filtering". In Proceeding of International Conference on Intelligent Transportation, Big Data & Smart City (ICITBS), 2018, pp. 262-265. IEEE.

[28] A. Garg and A. Negi, "Structure preservation in content-aware image retargeting using multi-operator". IET Image Processing, vol. 14, no. 13, pp.2965-2975, 2020.

[29] R. Singh, S. Nigam, A. K. Singh, and M. Elhoseny, "Wavelets and Intelligent Multimedia Applications: An Introduction". In Intelligent Wavelet Based Techniques for Advanced Multimedia Applications, 2020, pp. 1-12. Springer, Cham.

[30] Q. Liu, S. Yang, J. Liu, P. Xiong, and M. Zhou, "A discrete wavelet transform and singular value decomposition-based digital video watermark method". Applied Mathematical Modelling, vol. 85, pp.273-293, 2020.

[31] R. Bagaria, S. Wadhwani, and A. K. Wadhwani, "A Wavelet Transform and Neural Network Based Segmentation & Classification System for Bone Fracture Detection". Optik, p.166687, 2021.

[32] D. Patel and S. Raman, "Accelerated seam carving for image retargeting". IET Image Processing, vol. 13, no. 6, pp.885-895, 2019.

[33] Y. Chen, Y. Pan, M. Song, and M. Wang, ”Improved seam carving combining with 3D saliency for image retargeting“. Neurocomputing, vol. 151, pp.645-653, 2015.
[34] Y. Zhang, Z. Sun, P. Jiang, Y. Huang, and J. Peng, J., ”Hybrid image retargeting using optimized seam carving and scaling“. Multimedia Tools and Applications, vol. 76, no. 6, pp.8067-8085, 2017.
[35] Y. Zhou, Z. Chen and W. Li, "Weakly Supervised Reinforced Multi-Operator Image Retargeting," in IEEE Transactions on Circuits and Systems for Video Technology, vol. 31, no. 1, pp. 126-139, Jan. 2021, doi: 10.1109/TCSVT.2020.2977943.
[36] Garg, A., Negi, A. & Jindal, P. Structure preservation of image using an efficient content-aware image retargeting technique. SIViP, Vol. 15, pp. 185–193, 2021.

**Mohammad Reza Keyvanpour** is an Associate Professor at Alzahra University, Tehran, Iran. He received his B.Sc. in Software Engineering from Iran University of Science and Technology, Tehran, Iran. He received his M.Sc. and Ph.D. in Software Engineering from Tarbiat Modares University, Tehran, Iran. His research interests include Image Retrieval and Data Mining.

**Soheila Mehrmolaei** is received her B.Sc. in Software Engineering from Islamic Azad University, Mahshahr Branch, Iran. She is received M.Sc. in Computer Engineering at Islamic Azad University, Qazvin Branch, Iran. Her research interests include Time Series Mining, Artificial Intelligence, Image Processing, and Healthcare Time Series Analysis.

**Hoda sadaat Ahmadzadeh Hosseini** received her M.Sc. in Software Engineering from Alzahra University, Tehran, Iran. Her research interests include Image Processing and Data Mining.